Journal of Molecular Structure: THEOCHEM 862 (2008) 28–32

Contents lists available at ScienceDirect

Journal of Molecular Structure: THEOCHEM

journal homepage: www.elsevier.com/locate/theochem

Theoretical investigation on the mechanism and kinetics of toluene-OH adduct with oxygen molecule

Mingqiang Huang [a,b,*], Weijun zhang [a], Zhenya Wang [a], Liqing Hao [a], Wenwu Zhao [a], Xianyun Liu [a], Bo Long [a], Li Fang [a]

[a] Laboratory of Environment Spectroscopy, Anhui Institute of Optics and Fine Mechanics, Chinese Academy of Sciences, Hefei 230031, PR China
[b] Department of Environmental Science and Engineering, Xiamen University, Tan Kah Kee College, Xiamen 363105, PR China

ARTICLE INFO

Article history:
Received 15 May 2007
Received in revised form 19 April 2008
Accepted 21 April 2008
Available online 6 May 2008

Keywords:
2-Methyl-hydroxycyclohexadienyl radical
Oxygen molecule
Density functional theory
Reaction mechanisms
Transition states theory

ABSTRACT

A theoretical study of the mechanism and kinetics of the toluene-OH adduct I (2-methyl-hydroxycyclohexadienyl radical intermediate, generated from the reaction of OH with toluene) with O_2 is presented. The geometries of the reactants, transition states and products were optimized at B3LYP/6-31G(d,p) level. The single-point calculations for all the stationary points were carried out at the B3LYP/6-311++G (2df,2pd) level using the B3LYP/6-31G(d,p) optimized geometries. The results of the theoretical study indicate that the major product is o-cresol, and the minor product is the 2-methyl-hydroxycyclohexadienyl peroxyl radical V. And the overall rate constant for I and O_2 reaction is 5.21×10^{-16} cm^3 molecule^{-1} s^{-1} at the room temperature, showing a very good agreement with available experimental data. This study may provide useful information on understanding the mechanistic features of OH-initiated oxidation of toluene.

1. Introduction

It is well-known that aromatic compounds such as benzene, toluene, ethylbenzene, and xylenes (BTEX) are important constituents of automobile tailpipe exhaust and evaporative emissions [1,2]. In addition to their important role in photochemical ozone production, oxidation of aromatic compounds leads to formation of nonvolatile and semi-volatile organic compounds, which are responsible for secondary organic aerosol (SOA) in urban air [3]. Interest in SOA formation in the atmosphere has been renewed because of its possible impacts on the radiative balance associated with climate change [4], visibility degradation [5], and health effects [6].

Toluene is the most abundant aromatic atmospheric pollutant. Thus understanding the atmospheric chemistry of toluene is of great importance. It is well accepted that the most important removal process for toluene in the atmosphere is the reaction with OH. The OH-toluene reaction results in minor H-atom abstraction and major OH addition to the aromatic ring [7]. It has been well-established, both experimental [8] and theoretically [9–11], that OH addition to the ortho-position producing 2-methyl-hydroxycyclohexadienyl radical I is favored over the meta- and para-positions, regarding addition of OH to the benzene ring in toluene. Under atmospheric conditions, the radical I react with O_2 either by H-abstraction or by O_2 addition to form peroxy radicals. As shown in Fig. 1, H-abstraction operated by O_2 of hydrogen gem to OH in radical I, affording o-cresol. A new process has been recently repropounded, on the basis of the hypothesis put forward years ago by Shepson et al. [12]. This pathway would lead to the isomeric couple toluene oxide/oxepin (III and IV), via hydrogen abstraction from the hydroxyl in radical I operated by O_2. Several experimental studies have reported the rate constant of the O_2 with OH-toluene adduct. Early studies indirectly inferred this rate by fitting OH decay in the presence of toluene and O_2 and assuming a triexponential formulation and determined the rate constant of $(5–6) \times 10^{-16}$ cm^3 molecule^{-1} s^{-1} at the room temperature [13]. A more recent work by Bohn investigated the kinetics of the OH-toluene adduct with O_2 by monitoring the OH-adduct using cw UV-laser long path absorption and reported a larger rate constant of $(3 \pm 2) \times 10^{-15}$ cm^3 molecule^{-1} s^{-1} [14].

Several theoretical studies have been performed to investigate the structures and energetics of the intermediate radicals from the OH-initiated oxidation of toluene, providing further insight into the mechanism of the OH-toluene reactions. Bartolotti and Edney [15], Huang et al. [16], and Suh et al. [17] have performed theoretical investigations, looking at the initial attack of OH on toluene and subsequent addition reactions with O_2, using wavefunction- and density functional-based methods. These studies have shown that 2-methyl-hydroxycyclohexadienyl peroxy radical V is the most stable peroxy radicals. However, no investigations on the H-abstraction from the toluene-OH adduct are performed up to now. So, this paper will deal with those channels show in Fig. 1 that initiated from radical I. Reaction energies for the formation of the aromatic radicals were obtained to determine their relative

* Corresponding author. Tel.: +86 551 5591551; fax: +86 551 5591560.
E-mail address: huangmingqiang@gmail.com (M. Huang).

0166-1280/$ - see front matter © 2008 Elsevier B.V. All rights reserved.
doi:10.1016/j.theochem.2008.04.025

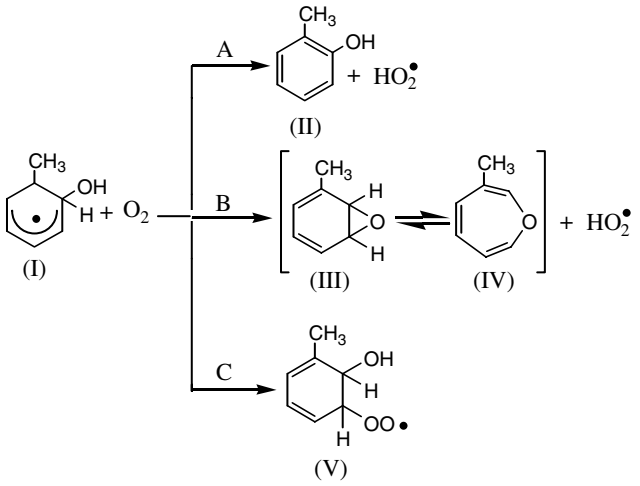

Fig. 1. Three postulated channel of toluene oxidation following OH addition to aromatic ring.

stability and reversibility, and activation barriers were analyzed to access the energetically favorable pathways to propagate the toluene oxidation. Kinetic calculations were performed using the classic transition state theory (TST) to assess the atmospheric degradation mechanism of the OH-toluene reaction system. Our theoretical results can provide useful information, complementary to the experimental results.

2. Computational methods

As pointed out by Schreiner et al. [18], DFT method has recently come under some serious disrepute especially concerning description of radicals, and MP2 often works better than DFT functionals especially when energies are concerned. In fact, as García-Cruz et al. [19] had noted, in several cases, that MP2 method consistently emphasizes the positive interactions in compounds where additions occurs on the substituted carbon atom on the ring. Moreover, MP2 method is impractical at this time due to the large size of the hydroxymethylcyclohexadienyl peroxy radicals molecule and the need for an open-shell treatment. However, B3LYP density functional method has already been validated in earlier studies on open-shell systems [11,17,20–22], For these systems, B3LYP results differed on average less than 1 kcal/mol from high-level ab initio calculations, and most often reproduced experimental barriers heights within 0.5 kcal/mol. Hence, we believe the B3LYP density functional method to be in general a reliable method for the calculations presented here. So all of the calculations were accomplished with the Gaussian 98 software package [23] using the B3LYP/6-31G(d,p) level of theory. The intrinsic reaction coordinate calculation (IRC) was employed to verify the relation that transition states connect reactants and products. The energies of all the reactants, transition states and products at the stationary points were improved by the single point energy calculations based on the B3LYP/6-31G (d,p) structures, using B3LYP/6-311++G(2df,2pd) method [24].

Rate coefficients were calculated applying to the transition state theory (TST) as implemented in The Rate program 1.0 [25]. According to the transition state theory under the condition of gas reaction, the rate constant, $k(T)$, is expressed by [26]

$$k(T) = \frac{k_B T}{h} \frac{Q_{TS}}{Q_R} e^{-E_a/K_B T}$$

where the Q are the partition functions of the transition states and the reactants and k_B is Boltzmann's constant, and E_a is the net activation energies.

The geometries of the reactants, transition states and products are shown in Fig. 2. The total energies and ZPE-corrected relative energies at B3LYP/6-311++G (2df,2pd)//B3LYP/6-31G(d,p) level of theory are listed in Table 1.

3. Results and discussion

Three possibly competing pathways were studied in their first step, to assess their relative feasibility (Fig. 1). All involve different reaction of O_2 with the 2-methyl-hydroxycyclohexadienyl radical intermediate I, which is taken as the reference in reporting energy differences. Begin either with abstraction operated by O_2 of hydrogen gem to OH in I, affording o-cresol (II, pathway A), or with O_2 addition to the π-delocalized system of I, producing 2-methyl-hydroxycyclohexadienyl peroxy radical intermediates (V, pathway C). Both appear to be very viable, with energy barriers of 4–7 kcal mol^{-1} (Table 1). In contrast, a recently repropounded pathway [12], which would lead to toluene oxide/oxepin, via hydrogen abstraction from the hydroxyl in I operated by O_2, appears not to be competitive, showing a significantly higher barrier (27 kcal mol^{-1}). Toluene oxide and oxepin are estimated to 18 and 16 kcal mol^{-1} lie above I respectively.

3.1. Pathway A

The transition structure corresponding to reaction A, TS-A is reported in Fig. 2. The transition vector (corresponding to an imaginary frequency of 201.4 cm^{-1}) is dominated by two contributions: the distance between the attacking oxygen and the hydrogen being abstracted and the distance between this hydrogen and the tetracoordinated carbon. However, comparison with some results obtained by Ignatyev et al. [27] in a theoretical study of the $C_2H_5 + O_2$ reaction could cast some doubts on a real nature of TS-A. In particular, the transition structure displayed in ref [27], relevant to a concerted elimination process in the ethylperoxy radical, must be considered. It can suggest that nature of TS-A might as well be that of a transition structure for HOO· elimination from one of the possible adducts of O_2 with I (namely, the one with O_2 bound to the ortho carbon, from the cycle face opposite to hydroxyl). Indeed, the distance of the terminal oxygen from the ortho carbon (OC) is not large, 2.496 Å, and compares with that of 2.200 Å, determined for elimination in the ethylperoxy radical. To better assess if TS-A is really relevant to the process of sheer H-abstraction from I, a standard IRC analysis was carried out. This computation yields a series of steps starting from the critical point, in a chosen direction. In the present case, the system was directed toward the still undetermined "reactant". On one hand, in both events (mere H-abstraction or concerted elimination), the system shift on the hypersurface would correspond to a lengthening of the HO distance and a shortening of the CH distance, because H-abstraction operated by one oxygen is part of the elimination process. On the other hand, the evolution of the HO distance, together with that of the OO bond length, could better help to clarify the matter. Indeed, if TS-A were originating from a peroxy adduct, OC should shorten (from 2.496 Å toward the adduct value of 1.503 Å), while the OO bond length would be stretched out (the values of 1.258 Å in TS-A and 1.323 Å in a peroxyl adduct provide a reference). In contrast, if TS-A derived from the O_2 and I moieties, its OC and OO should change in the opposite direction (OO = 1.214 Å in O_2). This test led to an unequivocal conclusion. As a result of a first series of twelve steps, OO underwent a shortening of 0.023 Å, at the same time OC was elongated by 0.043 Å.

The changes in the geometrical parameters relevant to the H transfer in the transition state with respect to reagents and products can be defined as Δ and Δ', respectively. They suggest in the

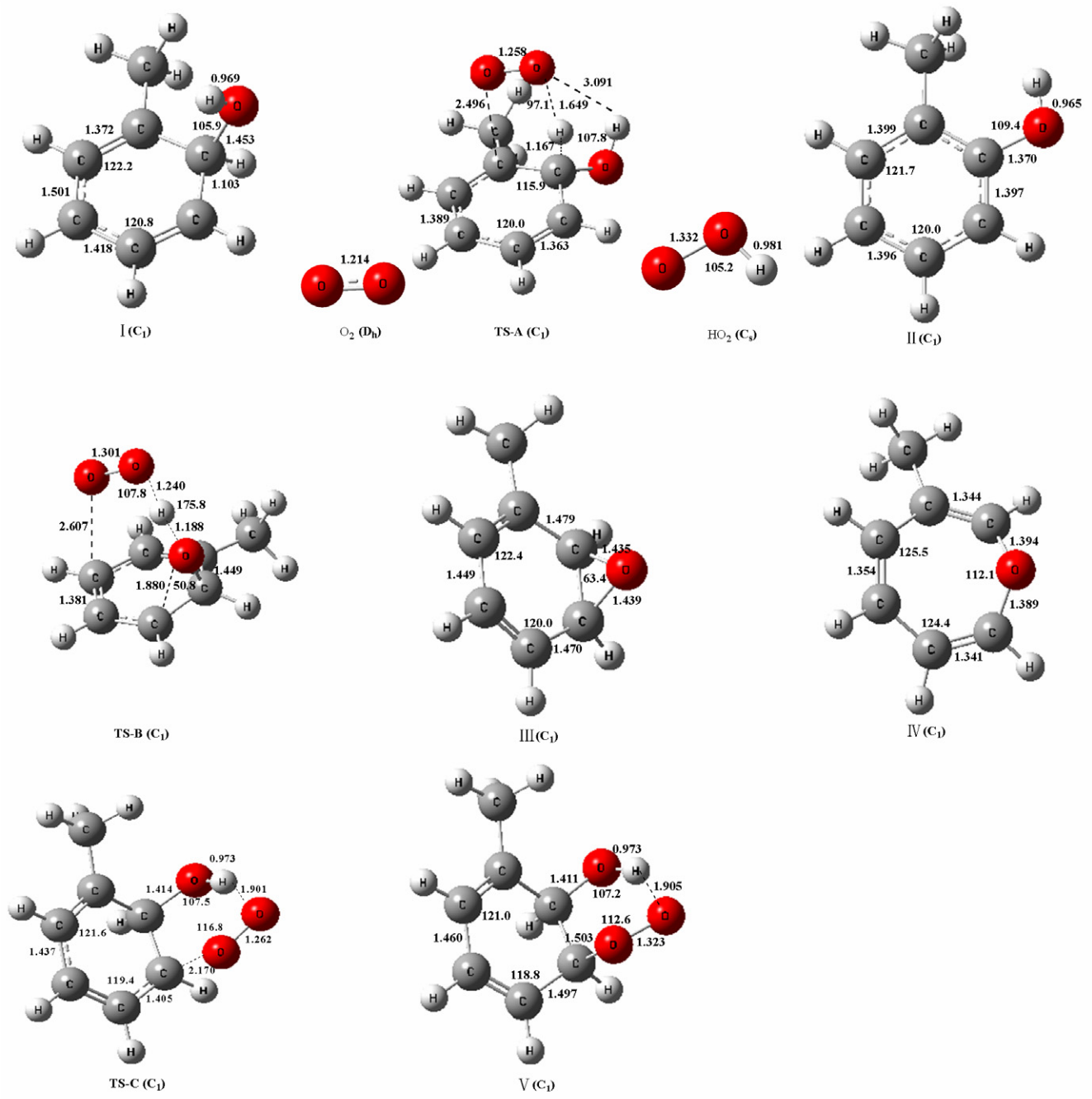

Fig. 2. Optimized geometries of the reactants, the intermediates and the products at the B3LYP/6-31G(d,p) level Bond length (Å) Bond angle (°).

present case a fairly early transition structure, consistent with the significant exothermicity (28.73 kcal mol^{-1}). In fact, ΔCH = +0.064 Å, while the O–H distance, 1.649 Å, is still larger than the final one (0.981 Å in HOO·). However, the change in OO bond is significantly more advanced: the increase of 0.040 Å from the initial value of 1.214 Å in O_2, being OO = 1.332 Å in HOO·. These variations describe a rather and asynchronous process.

3.2. Pathway B

The second process has been recently repropounded, on the basis of the hypothesis put forward years ago by Shepson et al. [12]. This pathway would lead to the isomeric couple toluene oxide/oxepin (III and IV), via hydrogen abstraction from the hydroxyl in I operated by O_2. The transition structure corresponding to reaction B, TS-B is reported in Fig. 2. This structure describes a concerted process. In fact, as the hydroxyl hydrogen is transferred, the oxygen bound to the cycle bends toward the ortho carbon, to close an epoxidic cycle. The transition vector (corresponding to an imaginary frequency of 1349.3 cm^{-1}) is dominated by the following contributions: the distance between the attacking oxygen and the hydrogen being abstracted and the distance between this hydrogen and the oxygen bound to the cycle; and one planar and one dihedral angle, relevant to the hydroxyl oxygen, which describe together its bending toward the ortho carbon. All these transition vector coefficients are again consistent with a concerted process. However, the variations in some important geometrical parameters suggest some asynchronicity in the transition structure

Table 1
The total energies (hartree) and ZPE-corrected relative energies (kcal mol^{-1}) of various species at the B3LYP/6-311++G(2df,2pd)//B3LYP/6-31G(d,p) level

Structure	Energy (hartree)	ZPVE[a] (hartree)	Relative energy (kcal mol^{-1})
I+O_2	−497.830738	0.139903	0.00
II+HO_2·	−497.877491	0.140872	−28.73
TS-A	−497.824917	0.139901	3.65
III+HO_2·	−497.802113	0.140366	18.25
IV+HO_2·	−497.804220	0.139632	16.47
TS-B	−497.786529	0.138033	26.57
V	−497.840331	0.144956	−2.85
TS-C	−497.821346	0.141749	7.05

[a] Scaled factor is 0.9614.

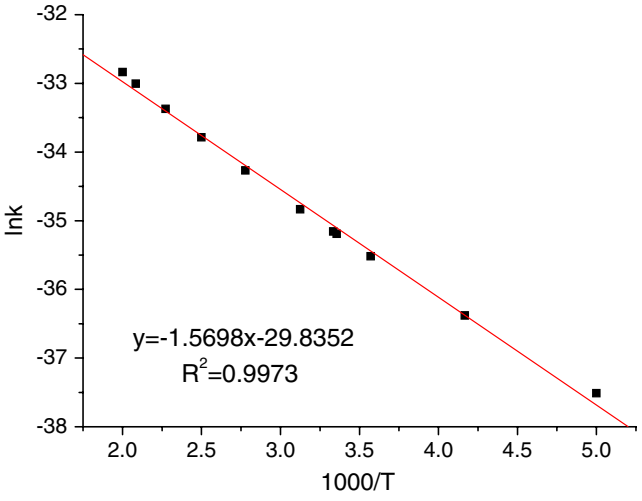

Fig. 3. Behavior of $\ln k_{overall}$ as a function of 1000/T in the 200–500 K range.

for this concerted process. These are the previously defined Δ and Δ' of the parameters OO (in dioxygen and HOO· radical), HO, and OH (relevant to H transfer), and the distance of the hydroxyl oxygen from the ortho carbon. Of these changes the following correspond to a rather transition structure, and are consistent with the endothermicity of the reaction (Table 1): ΔOO = 0.087 Å, Δ'OO = 0.031 Å and ΔOC_{ortho} = −0.547 Å, $\Delta' OC_{ortho}$ = −0.441 Å. In contrast, it can be noted that in Fig. 2: HO = 1.240 Å (Δ'HO = −0.259 Å) and OH = 1.188 Å (ΔOH = 0.219 Å). Thus, as mentioned above, the H transfer appears to be somewhat behind the other elementary processes, and suggests the idea of an asynchronous transition structure.

As was the case for TS-B, some small but favorable interaction keeps the terminal oxygen of the O_2 moiety rather close to the ring carbons. The shortest distance is that with the para carbon (2.607 Å). An IRC analysis, back in the direction of the "reactant", allows one to assess if TS-B is really relevant to the O_2H-abstraction process just described. Once again, if TS-B were an hydroyperoxyl elimination transition structure originating from a para peroxyl adduct, OC should shorten, tending to a value of ca. 1.503 Å, and the OO bond would undergo an elongation toward the value of 1.32 Å. In contrast, the result of a series of six steps shows OO undergoing a shortening of 0.047 Å, at the same time OC was elongated by only 0.012 Å.

3.3. Pathway C

The transition structure corresponding to reaction C, TS-C is reported in Fig. 2. The transition vector (corresponding to an imaginary frequency of 274.8 cm^{-1}) is dominated by a single contribution, the distance between the attacking oxygen and the carbon ortho to the tetracoordinated carbon. For reaction C, the changes in the more important geometrical parameters are as follows: Δ'CO = 0.667 Å, which corresponds to a value larger than the final one by +44% (1.503 Å in the adduct V), ΔOO = 0.048 Å, and Δ'OO = 0.061 Å. The last values would indicate again a rather early transition structure. However, the reaction step exothermicity is much more modest (Table 1). The result is consistent with the reversibility of the addition process observed experimentally [14].

Spin contamination is minimal using B3LYP. All energy minima show moderate contamination. The S^2 values are 2.0066 for O_2, 0.7876 for I, 0.7527 for HOO·, 0.7535 for the O_2 adduct V. The transition structures exhibit larger contaminations. The S^2 values are 1.0605 for TS-A, 0.7951 for TS-B, and 1.1670 for TS-C. In conclusion, both energy barrier and endothermicity indicate that pathway B is not favored with respect to the other two. These in turn present energy barriers of similar height (Table 1). It is apparent from data reaction A is not easily reversible, while C is. That oxygen addition was a reversible process that had already been observed in experimental studies [14].

Table 2
Partial and overall rate coefficients (cm^3 molecule^{-1} s^{-1}) as a function of temperature

T (K)	Path A	Path B	Path C	Overall
200	5.09×10^{-17}	2.27×10^{-41}	1.83×10^{-19}	5.11×10^{-17}
240	1.58×10^{-16}	6.94×10^{-37}	1.39×10^{-18}	1.59×10^{-16}
280	3.70×10^{-16}	1.51×10^{-33}	6.16×10^{-18}	3.76×10^{-16}
298	5.10×10^{-16}	1.71×10^{-32}	1.07×10^{-17}	5.21×10^{-16}
300	5.25×10^{-16}	2.26×10^{-32}	1.13×10^{-17}	5.36×10^{-16}
320	7.27×10^{-16}	3.09×10^{-31}	1.94×10^{-17}	7.46×10^{-16}
360	1.27×10^{-15}	2.45×10^{-29}	4.85×10^{-17}	1.32×10^{-15}
400	2.02×10^{-15}	8.29×10^{-28}	1.03×10^{-16}	2.12×10^{-15}
440	3.02×10^{-15}	1.51×10^{-26}	1.95×10^{-16}	3.22×10^{-15}
480	4.30×10^{-15}	1.72×10^{-25}	3.37×10^{-16}	4.64×10^{-15}
500	5.05×10^{-15}	5.04×10^{-25}	4.31×10^{-16}	5.48×10^{-15}

3.4. Kinetics

The calculation of the rate constants was performed using the program The Rate 1.0, in the 200–500 K temperature range. Results are listed in Table 2. Overall rate constant are also given. As can be observed in Table 2, the rate constant of Path A and C is about 10^{16} higher than Path B at 298 K. Path B can be negligible at the room temperature. The overall calculated rate constants for toluene-OH are plotted in Fig. 3 for the 200–500 K temperature range. The influence of temperature on the overall rate coefficient within this range has been interpreted in terms of the Arrhenius equation. An overall Arrhenius expression for the rate constant can be expressed as

$$k = 9.22 \times 10^{-17} e^{-119.3/RT}$$

And using the B3LYP/6-31G(d,p) we determined the overall rate constant of OH-toluene with O_2 is 5.21×10^{-16} cm^3 molecule^{-1} s^{-1}, showing a very good agreement with available experimental data reported by Knispel et al. [13]. The most recent study by Klotz et al. reported the o-cresol yield of 12.0 ± 1.4%, larger than any other oxidation product [8]. Hence the B3LYP/6-31G(d,p) method produces activation and reaction energies, rate constant of the toluene-OH reaction in good agreement with the experimental values.

4. Conclusion

The present theoretical results provide several new insights into the mechanism of toluene oxidation in the atmosphere. The first step of toluene oxidation is believed to see the formation of the so-called toluene-OH adduct I. Abstraction of the hydrogen gem to OH in I, operated by O_2, affords o-cresol, and O_2 addition to

the π-delocalized system of I, producing 2-methyl-hydroxycyclohexadienyl peroxy radical intermediate, appear to be very viable. Moreover, our work confirms previous experimental study on the reversibility of the reaction OH-toluene adduct with O_2. In contrast, a recently repropounded pathway, which would lead to toluene oxide/oxepin, via hydrogen abstraction from the hydroxyl in I operated by O_2, appears not to be competitive, showing a significantly higher barrier. And the overall rate constant for I and O_2 reaction is 5.21×10^{-16} cm^3 $molecule^{-1}$ s^{-1} at the room temperature, showing a very good agreement with available experimental data.

Acknowledgements

This work is supported by Knowledge Innovation Foundation of Chinese Academy of Sciences (KJCX2-SW-H08). The author thanks professors W.T. Duncan. R.L. Bell and T.N. Truong for providing The Rate programme through Internet.

References

[1] F.M. Black, L.E. High, J.M. Lang, J. Air Pollut. Control Assoc. 30 (1980) 1216.
[2] S. legett, Atmos. Environ. 30 (1996) 215.
[3] J.R. Odum, T.P.W. Jungkamp, R.J. Griffin, R.C. Flagan, J.H. Seinfeld, Science 276 (1997) 96.
[4] C. Pilinis, S.N. Pandis, J.H. Seinfeld, J. Geophys. Res. 100 (1995) 18739.
[5] A. Eldering, S.M. Larson, J.R. Hall, K.J. Hussey, G.R. Cass, Environ. Sci. Technol. 27 (1993) 626.
[6] J. Schwartz, D.W. Dockery, L.M. Neas, J. Air Waste Manag. Assoc. 46 (1996) 927.
[7] R. Atkinson, Atmos. Environ. 34 (2000) 2063.
[8] B. Klotz, S. Sorensen, I. Barnes, K.H. Becker, T. Etzkorn, R. Volkmer, U. Platt, K. Wirtz, M. Martin-Reviejo, J. Phys. Chem. 102 (1998) 10289.
[9] J.M. Andino, J.N. Smith, R.C. Flagan, W.A. William, J.H. Seinfeld, J. Phys. Chem. 100 (1996) 10967.
[10] V.H. Uc, I. Garcia-Cruz, A. Hernandez-Laguna, A. Vivier-Bunge, J. Phys. Chem. A 104 (2000) 7847.
[11] I. Suh, D. Zhang, R.Y. Zhang, L.T. Molina, M.J. Molina, Chem. Phys. Lett. 364 (2002) 454.
[12] P.B. Shepson, E.O. Edney, E.W. Corse, J. Phys. Chem. 88 (1984) 4122.
[13] R. Knispel, R. Koch, M. Sieze, C. Zetzsch, Ber. Bunsen-Ges. Phys. Chem. 94 (1990) 1375.
[14] B. Bohn, J. Phys. Chem. A 105 (2001) 6092.
[15] L.J. Bartolotti, O.E. Edney, Chem. Phys. Lett. 245 (1995) 119.
[16] M. Huang, W. Zhang, Y. Yang, Z. Wang, L. Hao, W. Zhao, W. Zhao, J. Li, X. Gao. J. Mol. Struct. (THEOCHEM) 774 (2006) 1.
[17] I. Suh, R.Y. Zhang, L.T. Molina, M.J. Molina, J. Am. Chem. Soc. 125 (2003) 12655.
[18] P.R. Schreiner, A.A. Fokin, R.A. Pascal, A. deMeijere, Org. Lett. 8 (2006) 3635.
[19] I. García-Cruz, M. Castro, A. Vivier-Bunge, J. Comput. Chem. 21 (2000) 716.
[20] J.J. Orlando, G.S. Tyndall, M. Bilde, C. Ferronato, T.J. Wallington, L. Vereecken, J. Peeters, J. Phys. Chem. A 102 (1998) 8116.
[21] L. Vereecken, J. Peeters, J. Phys. Chem. A 103 (1999) 1768.
[22] W. Lei, R. Zhang, J. Phys. Chem. A 105 (2001) 3808.
[23] M.J. Frisch, G.W. Trucks, H.B. Schlegel, G.E. Scuseria, M.A. Robb, J.R. Cheeseman, V.G. Zakrzewski, J.A. Montgomery Jr., R.E. Stratmann, J.C. Burant, S. Dapprich, J.M. Millam, A.D. Daniels, K.N. Kudin, M.C. Strain, O. Farkas, J. Tomasi, V. Barone, M. Cossi, R. Cammi, B. Mennucci, C. Pomelli, C. Adamo, S. Clifford, J. Ochterski, G.A. Petersson, P.Y. Ayala, Q. Cui, K. Morokuma, D.K. Malick, A.D. Rabuck, K. Raghavachari, J.B. Foresman, J. Cioslowski, J.V. Ortiz, A.G. Baboul, B.B. Stefanov, G. Liu, A. Liashenko, P. Piskorz, I. Komaromo, R. Gomperts, R.L. Martin, D.J. Fox, T. Keith, M.A. Allaham, C.Y. Peng, A. Nanayakkara, C. Gonzalez, M. Challacombe, P.M.W. Gill, B. Johnson, W. Chen, M.M. Wong, J.L. Andres, C. Gonzalez, M. Head-Gordon, E.S. Replogle, J.A. Pople, Gaussian 98 Revision A, Gaussian, Inc., Pittsburgh PA, 1998. 7.
[24] M.T. Nguyen, S. Creve, L.G. Vanquickenborne, J. Chem. Phys. 105 (1996) 1922.
[25] Shaowen Zhang, Thanh N. Truong, VKLab version 1.0, University of Utah, 2001.
[26] C. Eckart, Phys. Rev. 35 (1930) 1303.
[27] I.S. Ignatyev, X. Yaoming, D.A. Wesley, H.F. Schaefer, J. Chem. Phys. 107 (1997) 141.